Hindawi
Advances in Civil Engineering
Volume 2022, Article ID 7803002, 9 pages
https://doi.org/10.1155/2022/7803002

Research Article

The Effect of Length and Content of Fiber on Glass Fiber and Basalt Fiber-Reinforced Granite Residual Soil

Weijie Chen,[1] Jin Zhao,[1] Litao Fan,[1] Jia Li,[2] Bingxiang Yuan,[1] Hongzhong Li,[1] Guoping Jiang,[3] Hanbo Li,[4] and Tianying Chen[1]

[1]*School of Civil and Transportation Engineering, Guangdong University of Technology, Guangzhou 510006, China*
[2]*Company: Jiangmen Yinzhouhu Highway Co LTD, Transportation and Civil Engineering, Changsha University of Science and Technology, Changsha, China*
[3]*Fujian Jiangxia University, Fuzhou 350108, China*
[4]*Company: CCCC Fourth Navigation Bureau Second Engineering Co Ltd, Wuhan, China*

Correspondence should be addressed to Bingxiang Yuan; yuanbx@gdut.edu.cn

Received 30 May 2022; Accepted 20 June 2022; Published 15 July 2022

Academic Editor: Zhuo Chen

Fiber-reinforced soil boasts fewer cracks, higher energy absorption, and higher residual strength. With the well-established concept of carbon neutralization, it is necessary to reduce the dependence on high carbon-emitting reinforcement materials such as cement and concrete. The need for resource recycling has led to the development of reusing construction waste as the raw material for slope and embankment reinforcement. The purpose of this study is to analyze the reinforcement performance and environmental feasibility of glass and basalt fiber on granite residual soil with the content of 3%, 4%, and 5% and the length of 6 mm, 9 mm, and 12 mm. The reinforced samples were subjected to static impact load tests and SEM analysis to study its mechanical properties, microcharacteristics, and structure before and after reinforcement. Results show that the incorporation of 3% glass fibers of 6 mm has the best reinforcement effect on GRS, while the incorporation of 4% basalt fibers of 6 mm also has a good reinforcement ability. Glass fiber performs better than basalt fiber under the optimal content and length. SEM results indicate that glass fibers bind the soil particles more closely, thereby increasing their friction and leading to higher compressive strength. When the length and content of fiber exceed a certain range, the fibers are prone to cross and knot and fail to fill between soil particles, so the fiber and soil particles are separated, which lowers the strength of the soil. It is concluded that both glass fiber and basalt fiber can be well used for reinforcing GRS for higher bearing capacity and fewer cracks at the given proportion and length. Fiber length and content were considered when reinforcing GRS with different fibers in this study.

1. Introduction

With a skyrocketing population, the necessity of relieving traffic in urban areas and bolstering infrastructure construction has grown. Subway and infrastructure construction significantly alleviated traffic and satisfied people's demands, but it also inevitably generated a mass of waste soil, the treatment of which has become a matter of concern. It is predicted that China produced about 2 million tons of construction waste in 2019 alone [1]. Typically, the waste is removed by transportation and landfill. However, this traditional method is not sustainable, eco-friendly, or land-efficient; thus, the recycling of construction waste soil has become an important area of study.

In South China, the majority of construction waste consists of granite residual soil (GRS), which is produced under certain geographical conditions, climate, and geological environments. It is also known as a regionally distinctive soil due to its unique composition and structure [2–4]. Physical and chemical weathering crafted its distinctive structure with heterogeneity and anisotropy and its unique engineering geomechanical characteristics. Granite residual soil has good compressive properties in dry environment and unique structural properties, which include

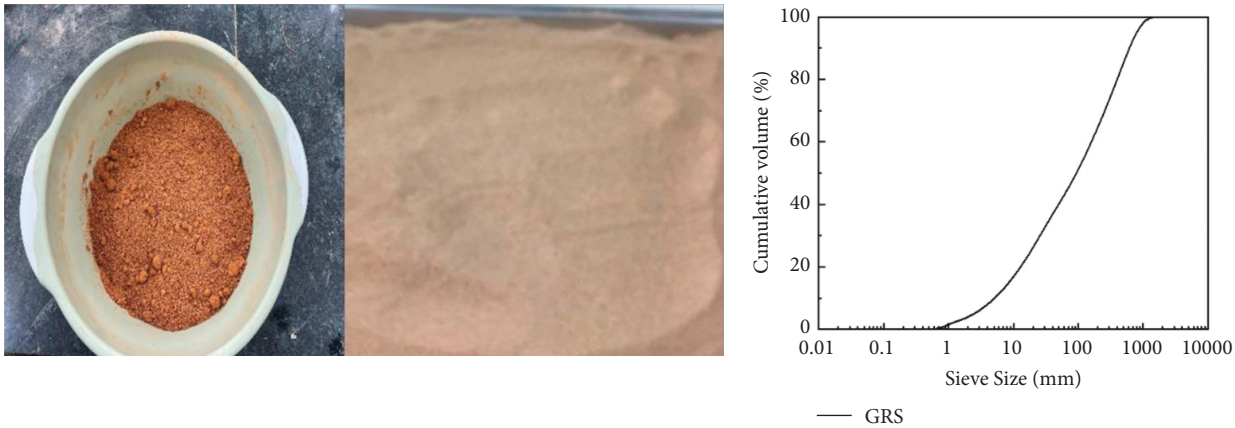

Figure 1: Material diagram. (a) Granite residual soil. (b) GRS particle size.

high void ratio, high strength, low density, and medium and low compressibility [5–9], rendering it a poor compressive material. This easily leads to a significant decrease reduction in bearing capacity after being saturated in water and a particularly sharp decline under dry-wet cycles, which in actual projects triggers natural disasters such as slope landslides and soil collapse. In reality, the majority of GRS is therefore treated as construction waste soil. For the recycling of GRS, the issue of its high porosity must be resolved, as it suggests restricted contact between soil particles [10–15]. Under external impact, bearing capacity tends to decline, resulting in incidents such as dislocation and sliding. Recycling GRS requires addressing its porosity.

Fibers, such as steel fiber, polyethylene fiber, and basalt fiber, are frequently employed in concrete engineering since it has been demonstrated that they effectively reduce the cracking of concrete and increase its tensile resistance under external load [16–19]. Therefore, some researchers utilized fibers to reinforce GRS. For instance, waste rubber fibers were mixed with swelling soil, and the mixture properties were studied by laboratory compaction test [20–24]. Results indicate that waste rubber fibers can considerably limit soil expansion and increase its resistance to cracking [25–27]. The modified swelling soil mixture is ideally suited for utilization as impervious liners and covers for urban solid waste landfills. Sisal fibers were incorporated into the soil, and the tensile properties of reinforced soils were investigated by indoor strength testing. Additionally, cement and cactus pulp were added to boost the strength [28–30]. The results demonstrated that cactus pulp, an environmentally benign natural ecological material, outperformed sisal fibers in reinforcing capacity. Apus bamboo root fibers were utilized to reinforce soil, and the shear strength behavior of the reinforced soil was analyzed using a direct shear test with a large box sample. The ratio of soil volume to root volume is proposed to quantify root density in soil mass [31]. The peak shear strength of reinforced soil was shown to improve as the soil-root volume ratio increased. Previous studies indicated that the impact resistance of GRS under dynamic load can be significantly improved by introducing SH solution and glass fiber. After reinforcing, the microscopic investigation revealed that the porosity was reduced and hydrophilic groups were replaced with hydrophobic groups, hence removing the hydrophilicity of GRS [32, 33].

Many authors have reported on fiber-reinforced GRS, with the majority focusing on fiber comparison. Little study has been conducted on the effect of fiber length and content. This study focuses on reinforcing GRS in an effective and economically viable manner, with environmental protection and sustainability as its central goals. The static load test was used to explore the reinforcing effect of glass and basalt fibers of varying lengths and contents, and SEM was used to analyze the reinforcement mechanism of GRS and the effect of fiber length and content from a microscopic perspective.

2. Experimental Study

2.1. Materials

2.1.1. Granite Residual Soil. Widely distributed in South China, granite residual soil is produced under specific geographical conditions, climates, and geological environments. Since it has special composition and structure, it is also called a regional special soil. The physical and chemical weathering made its distinctive structure with heterogeneity and anisotropy, and its unique engineering geomechanical characteristics. GRS often comprises yellowish-brown colors and mainly consists of cohesive soil, partly cobbly cohesive soil (Figure 1). This study adopted GRS from the Guangzhou area. The main geomechanical properties are given in Table 1.

2.1.2. Glass Fibers. As shown in Figure 2, the glass fiber used in the experiment is an inorganic nonmetallic transparent material with excellent performance. Glass fibers boast excellent performances, i.e., good insulation, heat resistance, corrosion resistance, and high mechanical strength. Glass fibers of 6 mm, 9 mm, and 12 mm in length were used as the reinforcer. The specific parameters of the glass fibers are shown in Table 2.

Table 1: Properties of granite residual soil samples.

Specific gravity, d_s	Water content, ω (%)	Density (g/cm^3)	Liquid limit, ω_l	Plastic limit, ω_p
2.67	13	16.5	48.3	27

(a) (b)

Figure 2: Material diagram. (a) Glass fiber. (b) Basalt fiber.

Table 2: Basalt fiber parameters.

Density (g/cm^3)	Linear density (dtex)	Elastic modulus (MPa)	Tensile strength (MPa)	Melting point (°C)	Elongation (%)
2.65	8.21	4500	330	958	3.0

Table 3: Glass fiber parameters.

Density (g/cm^3)	Linear density (dtex)	Elastic modulus (MPa)	Tensile strength (MPa)	Melting point (°C)	Elongation (%)
0.91	8.21	4286	346	169	36.4

2.1.3. Basalt Fiber. As shown in Figure 2, the basalt fiber used in this experiment is a continuous fiber made from natural basalt rock, composed of oxides including silicon dioxide, aluminum oxide, calcium oxide, magnesium oxide, ferric oxide, and titanium dioxide. Basalt continuous fiber is a new type of inorganic and green material with high performance including electrical insulation, corrosion resistance, and high-temperature resistance. Basalt fibers of 6 mm, 9 mm, and 12 mm in length were used as the reinforcer. The diameter of glass fiber is 14 μm, and the diameter of basalt fiber is 14–20 μm. The fiber data of this test are all provided by Taishan Fiber Co., Ltd. The specific parameters of the basalt fibers are given in Table 3.

2.2. Sample Preparation and Curing. The soil samples were baked in an oven at about 105°C for 6–8 h. The samples were removed out of the oven after they dropped to room temperature and then crushed and sieved (1.18 mm). The two fibers of different lengths and content were mixed with the soil samples evenly. According to the geotechnical specification [34], the GRS and fibers were prepared by layered sample preparation. First, the fibers and GRS were stirred evenly with a small electric mixer, then a small compactor was used for layered compaction, and the number of layers was 3 layers. A small compaction instrument was used to compact the samples into a cylinder with a diameter of 100 mm and a height of 50 mm (Figure 3) by adding the soils three times. The samples were air-dried in a ventilated and dry indoor place for 14 days. The sample weight is 1600 g.

2.3. Test Plan

2.3.1. Static Load Test. The optimal water content adopted in this study is 13% of existing research [32].

Fibers of different types, lengths, and contents were included in soil samples under the optimal water content, and the effects of different groups were studied through a static load test. The test plan is shown in Table 4.

The fiber content was kept at 3%, the optimal data from previous research, so only the effect of the length change of fiber is considered in this test.

Groups A, B, and C contain 3% glass fiber with a length of 6 mm, 9 mm, and 12 mm, respectively. As the reference, group 0 is GRS with no fiber. Other groups of the different mixtures are given in Table 4, and three samples were made for each variable.

2.4. Test Methods

2.4.1. Static Load Test. The uniaxial compressive strength of the samples was measured by a 4 W uniaxial compression

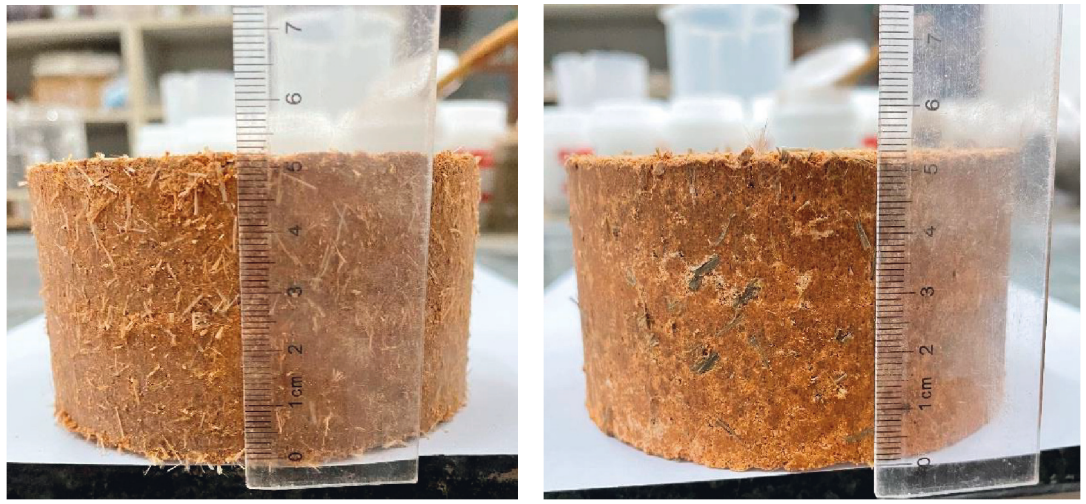

Figure 3: Reinforced glass fiber soil sample and reinforced basalt fiber soil sample.

Table 4: Static load test plan.

	Group	Sample name	Glass fiber (%)	Basalt fiber (%)	Length (mm)
Static load test	A	Glass fiber, 3%–6 mm	3	0	6
	B	Glass fiber, 3%–9 mm	3	0	9
	C	Glass fiber, 3%–12 mm	3	0	12
	D	Basalt fiber, 3%–6 mm	0	3	6
	E	Basalt fiber, 4%–6 mm	0	4	6
	F	Basalt fiber, 5%-6 mm	0	5	6
	G	Basalt fiber, 4%–9 mm	0	4	9
	H	Basalt fiber, 4%–12 mm	0	4	12
	O	0	0	0	0

test instrument (Figure 4). The samples were placed in the center of the bearing plate of the press to ensure that no eccentric loading occurs in loading. The loading rate was 0.5 MPa/s. The loading axial force when the sample failed was recorded to calculate the uniaxial compressive strength of each sample with the following formula [34]:

$$R = \frac{P}{A}. \quad (1)$$

R is the ultimate compressive strength of the sample, P is the maximum load when the sample failed, and A is the cross-sectional area of the sample.

The strength of the three samples under the same concentration was recorded. The strength values were averaged following the principle that the limit load does not exceed 10%. The reinforcement effect of fiber type, length, and content to GRS was investigated by a static load test. Aiming at achieving the optimal effect at a reasonable cost, the desired content and length of the two types of fiber were obtained in this study.

Figure 4: Uniaxial compression test instrument.

3. Results and Discussion

3.1. Static Load Test. The maximum stress of the soil sample without fiber was 850 kPa, and the corresponding strain value was 0.04% under static load as illustrated in Figure 5(a). From the data of groups A, B, and C as illustrated in Figure 5(b), the sample reinforced with glass fiber of 3% in content and 6 mm in length exhibited the best reinforcement performance of a maximum stress value of 1650 kPa, a corresponding strain value of 0.06% and a 94% increase of strength compared to fiberless samples. This finding signified that glass fiber can improve the compressive

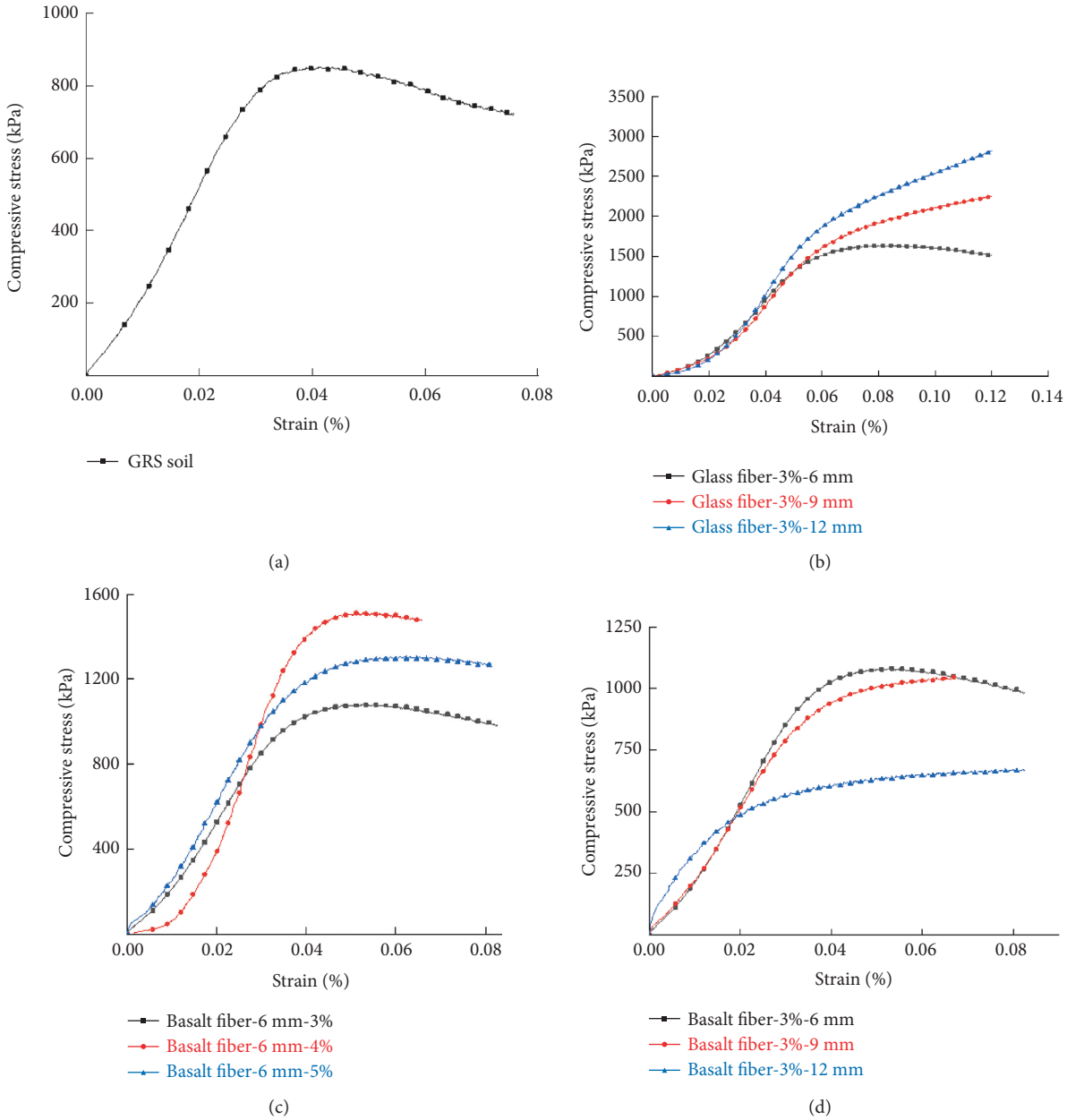

Figure 5: Continued.

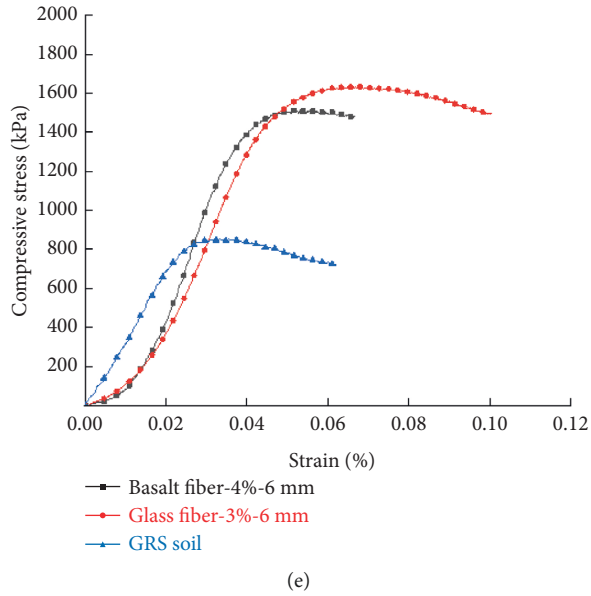

(e)

Figure 5: Compressive strength curve.

capacity of the sample. For samples of all three kinds of lengths, they went upward before the strain reached 0.05% and showed varied trends after that but before the strain reached 0.05%. An obvious trend of increase, peak, and decrease was observed in samples with 6 mm glass fibers, which peaked at 1650 kPa. However, samples with 9 mm and 12 mm glass fibers only showed a continuous upward trend. This result reveals that the incorporation of 6 mm glass fibers has a better reinforcement effect on GRS than 9 mm and 12 mm at the content of 3%. The reason behind this is that 6 mm glass fiber contacts with soil particles better and creates higher friction, enabling the sample to be more integrated and bear force together with fibers. The samples with 6 mm fiber had relatively reasonable deformation under the stress, and there is a corresponding relationship between strain and stress. By contrast, the stress of 9 mm and 12 mm samples increased with the strain continuously without peak or decline, indicating that the sample can be compressed and deformed infinitely and the stress can also increase infinitely, which is unreasonable. Therefore, it was concluded from the data that the reinforcement ability of the 6 mm glass fiber reinforcement effect was better than 9 mm and 12 mm under the same content of 3%.

From Figure 5(c), it is noticed that the samples with 6 mm basalt fibers at 3%, 4%, and 5% presented the maximum stress value of 900 kPa, 1500 kPa, and1300 kPa, respectively, 5%, 76%, and 53% higher than the fiberless sample. Thus, the inclusion of basalt fiber in GRS can improve its bearing capacity. In addition, the three curves all showed three stages: rise, peak, and fall. The strain value corresponding to the maximum stress value of the three was 0.05%. At a fixed length of 6 mm, the bearing capacity of the reinforced soil can be improved under the three content as proved in their curves and maximum stress values. To obtain a rather economical result, 3% basalt fibers showed a better reinforcement effect compared to 4% and 5% under the same length of 6 mm based on their maximum stress value and the corresponding strain value.

At a fixed basalt fiber proportion of 3%, the effect varied with lengths as illustrated in Figure 5(d), wherein the 6 mm sample performed the best as they reached a maximum stress value of 1100 kPa and a corresponding strain value of 0.05%, and the curve could be also divided into three stages of rising, peak, and fall. The curves of 9 mm and 12 mm length basalt fibers had a similar trend but only rose continuously.

The reason may be that a lower length of fiber means a larger quantity for the two kinds of fibers under the same content, so the fiber is distributed more evenly in the soil sample during preparation. At the initial stage of compression, the air and water in soil pores were expelled, and fiber processes higher elastic modulus compared to soil particles. Thus, the incorporation of fibers with lower length means more short fibers are distributed between soil particles, leading to higher friction and closer integration between soil and fiber, which is attributed to the higher compressive performance of the reinforced soil. However, long fiber in the soil is inclined to cross knot and overlap with each other, so the separation between the soil particles and fiber would occur under external load. Consequently, the fiber takes the force in place of the soil particles' stress, so the stress continued to increase with the strain without peak or downturn as shown in the figure. Thus, the optimum content and length of glass fiber are 3% and 6 mm and those of basalt fiber are 4% and 6 mm from the above data.

At the above optimal formula, the basalt and glass fiber reached a maximum stress of 1550 kPa and 1650 kPa and a corresponding strain of 0.05% and 0.06%, respectively, in Figure 5(e). The two kinds of fibers displayed an excellent effect on reinforcing GRS as an enhancement of the bearing capacity of GRS was achieved. GRS reinforced with 3% 6 mm glass fiber and 82% 6 mm basalt fiber witnessed a 94% and 82% strength increase, respectively. The results evidence that

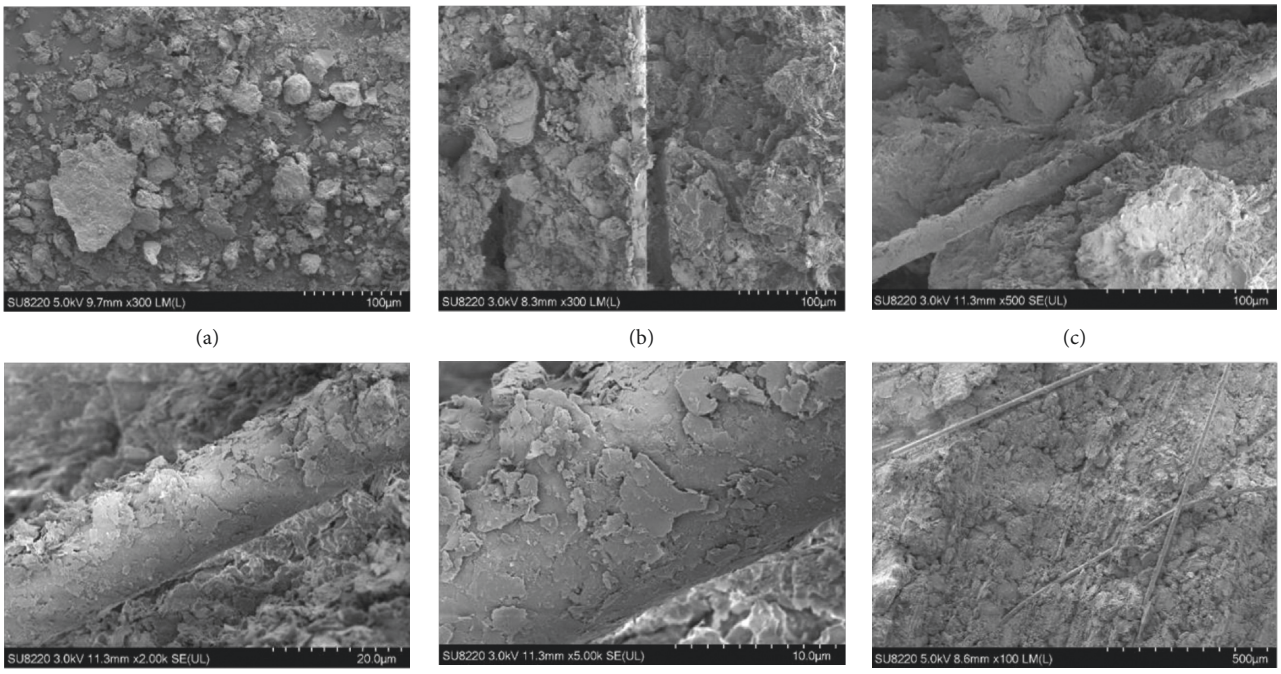

(a) (b) (c)

(d) (e) (f)

Figure 6: SEM of test soil.

glass fiber exhibited a better reinforcement effect than basalt fiber. The reason may be that glass fiber is finer than basalt fiber. As shown in Figure 2, glass fiber, a relatively fine cylinder as opposed to the flat basalt fiber, would find itself more easily filling in the pores of soil particles under the same length. The increased friction help enhance the integrity of the samples, which results in higher bearing capacity.

From the static load test analysis, it can be concluded that the reinforcement effect of glass fiber on granite residual soil is better than that of basalt fiber under the condition of optimal fiber content and length.

3.2. SEM. Given that the reinforcing ability of glass fiber is better than basalt fiber from the above mechanical analysis, the glass fiber samples were studied by SEM. The SEM images of samples taken from group O, group A, and group C after the static load test are given in Figure 6. At the magnification of 500x, the soil of control group O (Figure 6(a)) was granular particles with weak particle connection, so the sample failed under the impact of excessive static load. Compared with group O, the figures of group A (Figures 6(b)–6(e)) and group C (Figure 6(f)) show that the samples remained relatively intact under the impact load with glass fiber binding the soil into integration and jointly bearing the load. The glass fiber added to the soil acted as the reinforcer, which enhanced the integrity of the sample and its limit bearing capacity. It was noticed in Figures 6(d) and 6(e) that a considerable amount of soil particles were attached to the fiber, indicating that the inclusion of glass fiber into GRS can improve the friction and effective stress between soil particles and thus strengthen the soil. Based on the Mohr–Coulomb criterion of rock failure, when the failure occurs in the soil as a shear failure, the shear bearing capacity of soil fails to bear the shear stress produced by an external load. The shear stress-bearing capacity of soil lies in the friction force produced by the relative replacement of soil particles when sliding after compaction. Thus, the incorporation of glass fiber and basalt fiber increases the surface friction.

From Figure 6(f), it was revealed that fibers of excess length and content might cross and knot with each other and fail to contact the soil particles. Consequently, the soil particles and fibers were separated and failed to work together under the action of external load, so the effective stress of soil particles cannot be improved. Meanwhile, due to the separation of fibers and soil particles, the pores between soil particles are not filled with fibers. Therefore, adding fibers of excess length and amount cannot exhibit an excellent reinforcement effect, but may easily lead to a decline in bearing capacity.

SEM results show that, at appropriate length and content, fiber will be able to distribute well in the pores between soil particles, increase the internal friction force between soil particles, and attach to the surface of more soil particles. Fibers play a role alike to bridging and in connecting the soil particles around them, thus enhancing the integrity of the soil particles and helping maintain the intactness of the sample under external load.

4. Conclusion

In this study, a static load test was conducted on reinforced GRS to compare the reinforcing effect of glass and basalt fibers of different lengths and contents through group experiments. The influence of fiber's length and content and

the reinforcement mechanism were identified using the SEM technique:

(1) In static load tests, an enhancement in compressive strength is witnessed with the inclusion of the glass fiber and basalt fiber compared to fiberless samples, which proves the improvement effect of glass fiber and basalt fiber on the bearing capacity of GRS.

(2) The results of the static load test show that the incorporation of 6 mm basalt fiber exhibited the best reinforcement effect with a maximum stress of 1100 kPa among samples containing 3% basalt fiber. Moreover, the incorporation of 4% basalt fiber exhibited the best reinforcement effect with a maximum stress of 1550 kPa among samples containing 6 mm basalt fiber. Hence, the optimal length and content of basalt fiber are 6 mm and 4%. The optimal length and content of glass fiber are 6 mm and 3% based on the data.

(3) At the above optimal formula, the basalt and glass fiber reached a maximum stress of 1550 kPa and 1650 kPa and a corresponding strain of 0.05% and 0.06%. Re-SEM analysis indicates that fibers are prone to cross and knot and fail to fill between soil particles when the length and content of the fiber exceed a certain range, which lowers the integration between them and lowers the bearing capacity of the soil.

(4) SEM analysis indicates that fibers are prone to cross and knot and fail to fill between soil particles when the length and content of fiber exceed a certain range, which lowers the integration between them and lowers the bearing capacity of the soil.

Data Availability

Data can be obtained from the corresponding author upon request.

Conflicts of Interest

The authors declare that they have no conflicts of interest.

Acknowledgments

The authors would gratefully like to acknowledge the support provided by the National Natural Science Foundation of China (nos. 51978177 and 41902288).

References

[1] S. Nanda and F. Berruti, "Municipal solid waste management and landfilling technologies: a review," *Environmental Chemistry Letters*, vol. 19, pp. 1433–1456, 2020.

[2] Y. He, F. Gu, C. Xu, and Y. Wang, "Assessing of the influence of organic and inorganic amendments on the physical-chemical properties of a red soil (Ultisol) quality," *Catena*, vol. 183, Article ID 104231, 2019.

[3] Y. Deng, X. Duan, S. Ding, C. Cai, and J. Chen, "Suction stress characteristics in granite red soils and their relationship with the collapsing gully in south China," *Catena*, vol. 171, pp. 505–522, 2018.

[4] J. Xia, C. Cai, Y. Wei, and X. Wu, "Granite residual soil properties in collapsing gullies of south China: spatial variations and effects on collapsing gully erosion," *Catena*, vol. 174, pp. 469–477, 2019.

[5] W. Chen, Z. Chen, and S. Liu, "EXPERIMENTAL RESEARCH ON STRESS PATHS OF GRANITE RESIDUAL SOIL," *Industrial Construction*, vol. 47, pp. 11–16, 2017.

[6] B. Bai, Y. Wang, D. Rao, and B. Fan, "The effective thermal conductivity of unsaturated porous media deduced by pore-scale SPH simulation," *Frontiers of Earth Science*, 2022.

[7] B. Bai, Q. Nie, ZhangYike, X. Wang, and W. Hu, "Cotransport of heavy metals and SiO2 particles at different temperatures by seepage," *Journal of Hydrology*, vol. 597, Article ID 125771, 2021.

[8] B. Bai, R. Zhou, G. Cai, W. Hu, and G. Yang, "Coupled thermo-hydro-mechanical mechanism in view of the soil particle rearrangement of granular thermodynamics," *Computers and Geotechnics*, vol. 137, no. 8, Article ID 104272, 2021.

[9] B. X. Yuan, M. J. Chen, W. J. Chen, Q. Luo, and H. z. Li, "Effect of pile-soil relative stiffness on deformation characteristics of the laterally loaded pile," *Advances in Materials Science and Engineering*, 2022.

[10] X. Liu, X. Zhang, L. Kong, G. Wang, and H. Li, "Formation mechanism of collapsing gully in southern China and the relationship with granite residual soil: a geotechnical perspective," *Catena*, vol. 210, Article ID 105890, 2022.

[11] H. Mei, X. Jian, W. Zhang, H. Fu, and S. Zhang, "Behavioral differences between weathering and pedogenesis in a subtropical humid granitic terrain: implications for chemical weathering intensity evaluation," *Catena*, vol. 203, Article ID 105368, 2021.

[12] F. Ferreira, C. Vieira, and M. De, "Cyclic and post-cyclic shear behaviour of a granite residual soil -geogrid interface," *ADVANCES IN TRANSPORTATION GEOTECHNICS III*, pp. 379–386, 2016.

[13] Y. Peng, S. Tang, J. Huang, C. Tang, L. Wang, and Y. Liu, "Fractal analysis on pore structure and modeling of hydration of magnesium phosphate cement paste," *Fractal Fract*, vol. 6, p. 337, 2022.

[14] L. Wang, Z. Yu, B. Liu, F. Zhao, S. Tang, and M. Jin, "Effects of fly ash dosage on shrinkage, crack resistance and fractal characteristics of face slab concrete," *Fractal Fract*, vol. 6, p. 335, 2022.

[15] L. Wang, G. Li, X. Li et al., "Influence of reactivity and dosage of MgO expansive agent on shrinkage and crack resistance of face slab concrete," *Cement and Concrete Composites*, vol. 126, Article ID 104333, 2022.

[16] D. Kar, "Properties, Applications: Slurry Infiltrated Fiber Concrete (SIFCON)," *Concrete International*, 1984.

[17] H. Y. Yang, J. Li, Q. Z. Ye, and X. C. Zhang, "Research on absorbing EMW properties of steel-fiber concrete," *Journal of Functional Materials*, 2002.

[18] S. Acostacalderon, P. Gordillosilva, V. B. Dan, and J. F. Rada, "Comparative Evaluation of Sisal and Polypropylene Fiber Reinforced Concrete Properties," *FIBERS*, 2022.

[19] A. Tibebu, E. Mekonnen, L. Kumar, J. Chimdi, H. Hailu, and N. Fikadu, "Compression and workability behavior of chopped glass fiber reinforced concrete," *Materials Today Proceedings*, 2022.

[20] S. S. Narani, M. Abbaspour, S. M. M. M. Hosseini, E. Aflaki, and F. M. Nejad, "Sustainable reuse of Waste Tire Textile

Fibers (WTTFs) as reinforcement materials for expansive soils: with a special focus on landfill liners/covers," *Journal of Cleaner Production*, vol. 247, no. C, Article ID 119151, 2020.

[21] B. Yuan, Z. Li, Z. Zhao, H. Ni, Z. Su, and Z. Li, "Experimental study of displacement field of layered soils surrounding laterally loaded pile based on Transparent Soil," *Journal of Soils and Sediments*, vol. 21, pp. 3072–3083, 2021.

[22] B. Yuan, S. Meng, X. Lei, Q. Luo, P. S. Prasad, and H. z. Li, "Investigation of 3D deformation of transparent soil around a laterally loaded pile based on a hydraulic gradient model test," *Journal of Building Engineering*, vol. 28, no. 3, Article ID 1010124, 2020.

[23] B. Yuan, M. Sun, Y. Wang, L. Zhai, Q. Luo, and X. Zhang, "Full 3D displacement measuring system for 3D displacement field of soil around a laterally loaded pile in transparent soil," *ASCE International Journal of Geomechanics* no. 5, Article ID 04019028.

[24] B. Yuan, Z. Li, Z. Su, Q. Luo, M. Chen, and Z. Zhao, "Sensitivity of multistage fill slope based on finite element model," *Advances in Civil Engineering*, Article ID 6622936, 2021.

[25] P. S. Narayanan, "Study on Shear Parameters of Waste Tire Rubber Fiber Mixed Cohesionless Soil by Series of Triaxial Tests," *International Journal of Advanced Scientific and Technical Research*, 2015.

[26] B. Yuan, L. Zihao, W. Chen et al., "Xudong. Influence of groundwater depth on pile–soil mechanical properties and fractal characteristics under cyclic loading," *Fractal and Fractional*, vol. 6, no. 4, p. 198, 2022.

[27] B. Yuan, L. Xiong, L. Zhai et al., "Transparent synthetic soil and its application in modeling of soil-structure interaction using optical system," *Frontiers of Earth Science*, vol. 7, p. 276, 2019.

[28] R. Mattone, "Sisal fibre reinforced soil with cement or cactus pulp in bahareque technique [J]," *Cement and Concrete Composites*, vol. 27, no. 5, pp. 611–616, 2004.

[29] P. V. Joseph, K. Joseph, and S. Thomas, "Effect of processing variables on the mechanical properties of sisal-fiber-reinforced polypropylene composites," *Composites Science and Technology*, vol. 59, no. 11, pp. 1625–1640, 1999.

[30] G. Xiang, D. Song, and Z. Chen, "Investigated stress-strain relationships of municipal solid waste incineration bottom ash," *Geomatics, Natural Hazards and Risk*, vol. 11, no. 1, pp. 2431–2448, 2020.

[31] M. F. Ma'Ruf, "Shear strength of Apus bamboo root reinforced soil," *Ecological Engineering*, vol. 41, pp. 84–86, 2012.

[32] B. Yuan, L. Zihao, C. Yiming et al., "Mechanical and microstructural properties of recycling granite residual soil reinforced with glass fiber and liquid-modified polyvinyl alcohol polymer," *Chemosphere*, vol. 286, no. P1, Article ID 131652, 2022.

[33] B. X. Yuan, W. J. Chen, J. Zhao, F. Yang, Q. Luo, and T. Chen, "The effect of organic and inorganic modifiers on the physical properties of granite residual soil," *Advances in Materials Science and Engineering*, 2022.

[34] "GB/T 50123-2019," *Standard for Geotechnical Testing Method*, 2019.